Chapter 8

Vanadyl Phosphate Nano sheets-MWCNT Composite Free standing thin film For Supercapacitor Application

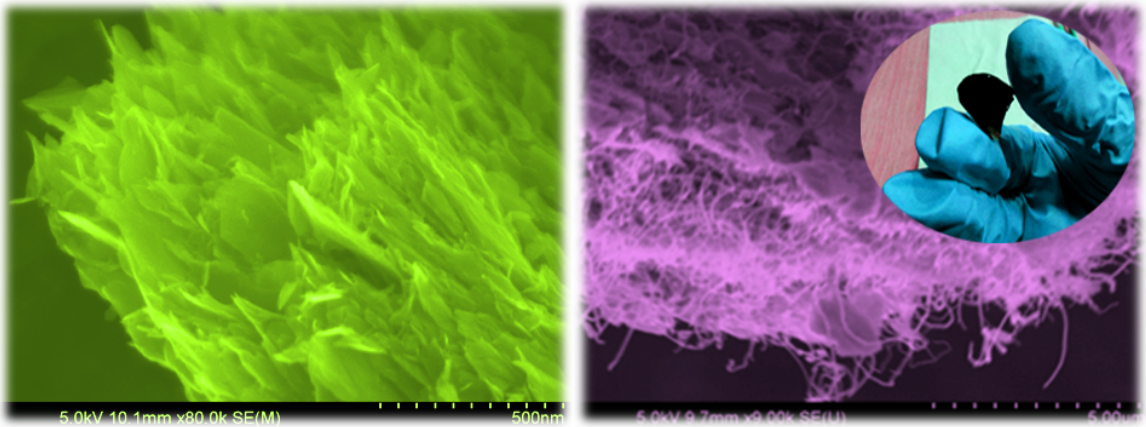

Work presented in this chapter has been published in:

AIP Conf. Proc., 2016, 1728, 020479

Shibsankar Dutta, Sukanta De.

8.1. Introduction

It have been already seen that 2-dimensional nano materials are the suitable choice for the supercapacitor application due to their large specific surface area, electrochemical active sites, micromechanical flexibility, expedite ion migration channel properties. This chapter enlightens free standing hybrid films of functionalized MWCNT (–COOH group) and α-Vanadyl phosphates ($VOPO_4{\cdot}2H_2O$), prepared by vacuum filtering.

The performance of supercapacitor directly depends on the electrode materials. Therefore to improve the electrochemical performance of supercapacitor we need to develop new electrode materials with high capacitance behavior relative to the existing electrode materials for supercapacitor in the market. Till now active carbon material like carbon aerogels, Carbon nanotubes, reduced grapheme oxide etc. are widely used electrode materials due to the porous texture, high electrical conductivity, high specific surface area, good mechanical and thermal stability[3]. However the carbon based electrode materials have some limitation like high cost, low energy storage mechanism[4].To enhance the performance of supercapacitors inorganic metal oxides, sulphides, conducting polymers, transition metal phosphate were introduced as an electrode material, and the hybrid electrode materials enhanced the electrochemical performance due to the balanced of high specific surface area and high electrical conductivity[5]. S.L. Chou and co-workers has developed a novel electrode material MnO_2 nanowires over CNT paper, obtained the specific capacitance 167.5 F/ g at 77 mA/ g [6]. X. Lu et al. already reported CNT @V_2O_5 nano wire composite electrode materials resulting high specific capacitance 57.3 F/ g[7]. J. Ge and co-workers reported SWNT film on PET substrate as an electrode material, resulting specific capacitance 55.0 F/g at 2.6 A/ g[8]. Among these electrode materials (MnO_2,V_2O_5, MoS_2, MoO_3, RuO_2,$VOPO_4$ etc.) RuO_2 electrode obtained highest specific capacitance, but due to high cost, low abundance, high toxicity we need alternative electrode materials which also perform like RuO_2 electrode material.

Among all of the alternative candidates for supercapacitor transition metal phosphates like vanadyl phosphate dihydrate ($VOPO_4$, $2H_2O$) have attained the attention due to high voltage upto 3.5 V, low cost and most importantly due to their environmental friendliness. Vanadyl phosphate dihydrate offered high potential compared to the oxides due to the peculiar layered structure in which V-O-P layers forms due to the

corner sharing oxygen atom of PO_4 tetrahedral and VO_6 octahedral.[8,9] However, the conductivity of $VOPO_4.2H_2O$ is small compared to the other metal oxides and it plays a major drawback to the practical application.[9,10]Overcoming these limitations, we introduce a novel electrode material hybrid of $VOPO_4$ nanosheets and MWCNT in the present work.$VOPO_4$ nanosheets enhanced the electrochemical behavior because of their large specific surface area, high micromechanical flexibility, extra electrochemical active sites and MWCNT enhanced the electrical conductivity of the electrode materials.

8.2 Experimental

8.2.1. Synthesis of bulk vanadyl phosphate dehydrate

Bulk vanadyl phosphate dihydrate ($VOPO_4{\cdot}2H_2O$) was prepared according to the previously reported literature[10]. 12gm V_2O_5 was added to the mixture of 68 ml H_3PO_4 and 290 ml DI water and refluxed at 110^0C for 16 h. Finally the yellow precipitate was collected by vacuumed filtration and thereafter the resulting sample was washed by DI water and Acetone several times and dried in vacuum at 60^0C.

8.2.2. Exfoliation of bulk $VOPO_4{\cdot}2H_2O$

Bulk vanadyl phosphate dihydrate was dispersed into 2 propanol with an initial concentration 1mg/ml[10]. Thereafter the dispersion was ultrasonicated by bath sonication for 15 minutes to get vanadyl phosphate nanosheets, the resulting well dispersed nanosheets were used to make composite films.

8.2.3. MWCNT@$VOPO_4{\cdot}2H_2O$ hybrid film

Initially commercially available MWCNT was dispersed into 2 propanol with bath sonication as previously reported literature.[11] Further, the dispersed solutions of MWCNT and $VOPO_4{\cdot}2H_2O$ were added together and sonicated for couple of minutes to get well dispersed mixture of both. MWCNT-Vanadyl phosphate hybrid films were prepared by filtering an appropriate amount of mixed dispersion through polyvinylidene fluoride (PVDF) filtration membrane (Millipore, Durapore membrane filters, and 100 nm pore size). The deposited hybrid films were dried overnight under vacuum at 50^0C. Films were peeled off the filter membrane to get free standing hybrid films for detailed characterization.

8.3. Characterization

X-ray diffraction (XRD) analysis of powder sample was performed using a X-RAY DIFFRACTOMETER (XRD) Bruker D8. Raman spectra were recorded at room temperature with a Confocal Raman Microscope.Surface morphology was investigated with field emission scanning electron microscope (FESEM, HITACHI S-4800). The TEM images were taken on a JEOL-2010 transmission electron microscope instrument using an acceleration voltage of 200 kV. Cyclic voltammetry (CV) and galvanostatic charge–discharge tests were performed using an electrochemical analyzer (CHI660E) with two electrode cell using 1 M Na_2SO_4 as electrolyte.

8.4. Results and discussion

8.4.1. Structural & morphological analysis:

We have done powder X-ray diffraction (XRD) and Raman study to characterize as prepared $VOPO_4{\cdot}2H_2O$. As shown in Fig.8.1(a), the X-ray diffraction pattern of as prepared vanadyl phosphate dihydrate shows a set of diffraction peaks at $2\theta = 12.3^0$, $24.9^0$and 28.7^0 corresponding to (001),(002) and (102) planes with d values 0.71nm,0.36 nm,0.32 nm respectively. The formation of α phase of $VOPO_4{\cdot}2H_2O$ have confirmed from the XRD (JCPDS card No.84-0111) pattern.

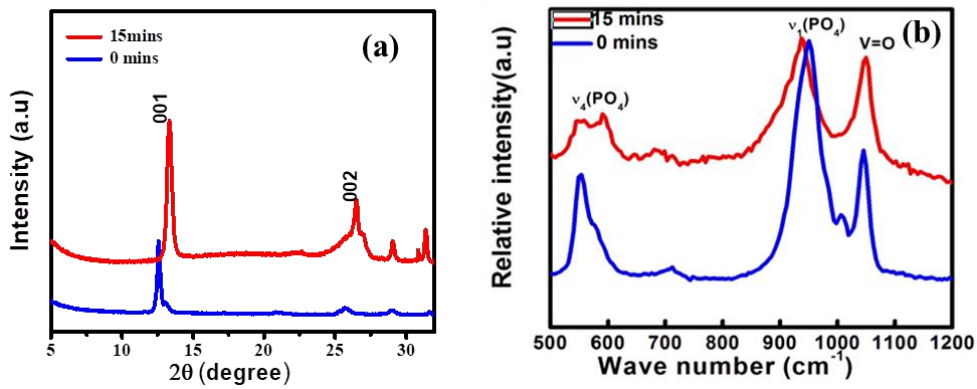

Figure8.1. (a) Powder XRD pattern and (b) Raman spectra of as prepared and exfoliated $VOPO_4{\cdot}2H_2O$

The relatively stronger (001) peak after exfoliation conforms formation of 2D $VOPO_4$ nanosheets. Moreover, shift of the (001) peak from lower 2θ (12.51°) to a higher (13.28°) during exfoliation, indicating the reduction of the interlayer spacing between two $VOPO_4$ layers, because of escape of H_2O molecules from interlayers.

The band at 950 cm^{-1} in the Raman spectrum (Fig.8.1b) for as prepared $VOPO_4 \cdot 2H_2O$ is corresponds to symmetric stretching vibration $\nu_1(PO_4)^{12}$ which shifted to lower wave number at 937 cm^{-1} for exfoliated $VOPO_4$. This shift is due to breaking of hydrogen bonds from oxygen atoms of the P-O bond in $VOPO_4$. The bands due to symmetric bending vibrations $\nu_4(PO_4)$ at 550 and 580 cm^{-1} also present in Raman spectrum for both as prepared and exfoliated vanadyl phosphate. The band at 1050 cm^{-1} is corresponding to V=O stretching mode. The Raman spectra confirmed that there is no obvious change in in–plane structure of $VOPO_4$.

Transmission electron microscopy (TEM) image of the exfoliated $VOPO_4$ nanosheets were taken on lacy carbon coated copper grid. Thin sheet like structures of $VOPO_4$ was observed under TEM (Fig.8.2a). Figure 8.2(b) shows the EDX pattern of $VOPO_4$ in which intense peaks observed corresponding to elements V, P and O.

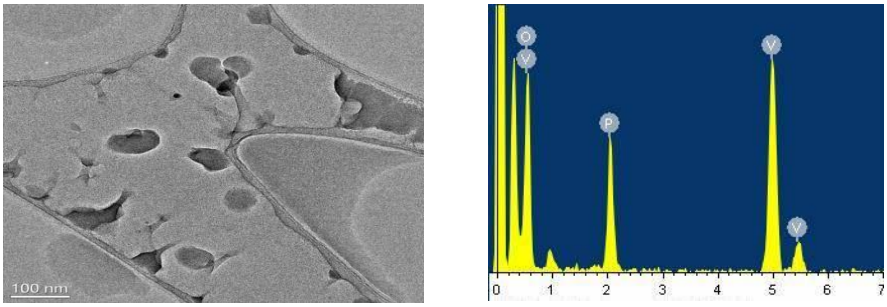

Figure 8.2. Low magnification TEM image (a) and EDX spectra (b) of $VOPO_4$ nanosheet

Scanning electron microscopy (SEM) was used to study the morphology of exfoliated $VOPO_4$ and the composite films. Shown in Figure 8.3(a) is a SEM image of exfoliated $VOPO_4$ which shows graphene like morphology of $VOPO_4$ after 15 mints sonication in 2 propanol. Figure 8.3(b) shows the FESEM image of MWCNT-$VOPO_4$ composite. This clearly shows the excellent mixing of $VOPO_4$ nanosheets into the MWCNT network and is uniformly distributed.

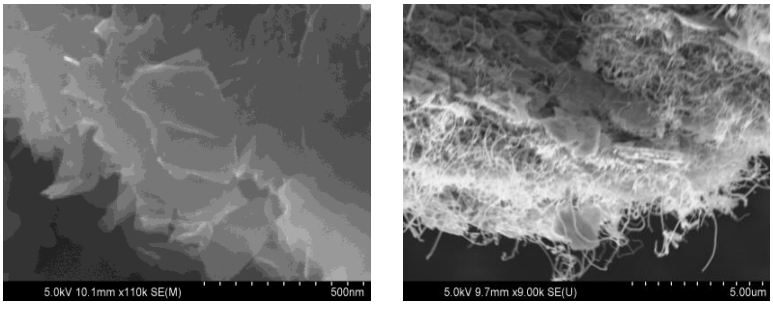

Figure 8.3.FESEM images of $VOPO_4$ nanoshees (a), $VOPO_4$/MWCNT (b)

8.4.2. Electrochemical Study:

To evaluate the performance of MWCNT-$VOPO_4$ hybrid films as electrode of supercapacitor, we have performed cyclic voltammetry (CV), galvanostatic charge-discharge (CD), and electrochemical impedance spectroscopy (EIS) tests using a two-electrode system. Figure 8.4(a) shows the CV curves of hybrid electrodes at different scan rates 5mV/s to 100 mV/s with a voltage window (-2.4 V to +2.4V). Redox peaks are observed in CV curve at about (+/-) 1V. CV measurements of pure MWCNT electrode are also tested which reveals the performance of hybrid electrode over the pure MWCNT electrode (Fig.8.4b). The charge storage mechanism of the electrode can be shown by the following reversible equation[13]

$$VO^{3+} + e^{-} + H^{+} = HVO^{3+}$$

The specific capacitance values calculated from the CV curves to be 236, 179, 87, and 59 F/g at 5, 10, 50, and 100 mV/sec scan rates respectively for hybrid materials. However the value of specific capacitance for pure MWCNT electrode at 5 mV/sec scan rate is 49 F/g. From the charging discharging curves(Fig 8.4c) and (Fig 8.4d) the value of specific capacitance of pure MWCNT electrodes and hybrid electrodes were found to be 3F/g and 82 F/g at current density 1 A/g respectively. Specific capacitance calculated from CV curve for hybrid film is almost five times higher than that of MWCNT only film.

Further to evaluate the energy efficiency of supercapacitor based on hybrid materials of MWCNT-$VOPO_4$, energy density (E) and power density (P) were calculated from the CD curves in figure 4, using the equations $E = \frac{1}{2}CV^2$ and $P = \frac{E}{\Delta t}$, where C is the specific capacitance, V is the working voltage and Δt is the discharging time. Here we use the capacitance values calculated from CD curve. The supercapacitor based on hybrid materials deliver a high energy density of 65.6 Wh/Kg at a power density 1476 W/Kg which is superior to previously reported hybrid materials consist of 2D nanomaterials and carbon nanostructure[14,15]. From SEM image of hybrid film (Figure 8.3C), we have observed the excellent mixing of VOPO4 nanosheets into the MWCNT network and uniform distribution which should facilitate charge transport throughout the electrode and also mesoporous structure of hybrid allow access of electrolyte to the

internal surface. This could be one reason of superior performance of supercapacitor based on MWCNT-$VOPO_4$ hybrid.

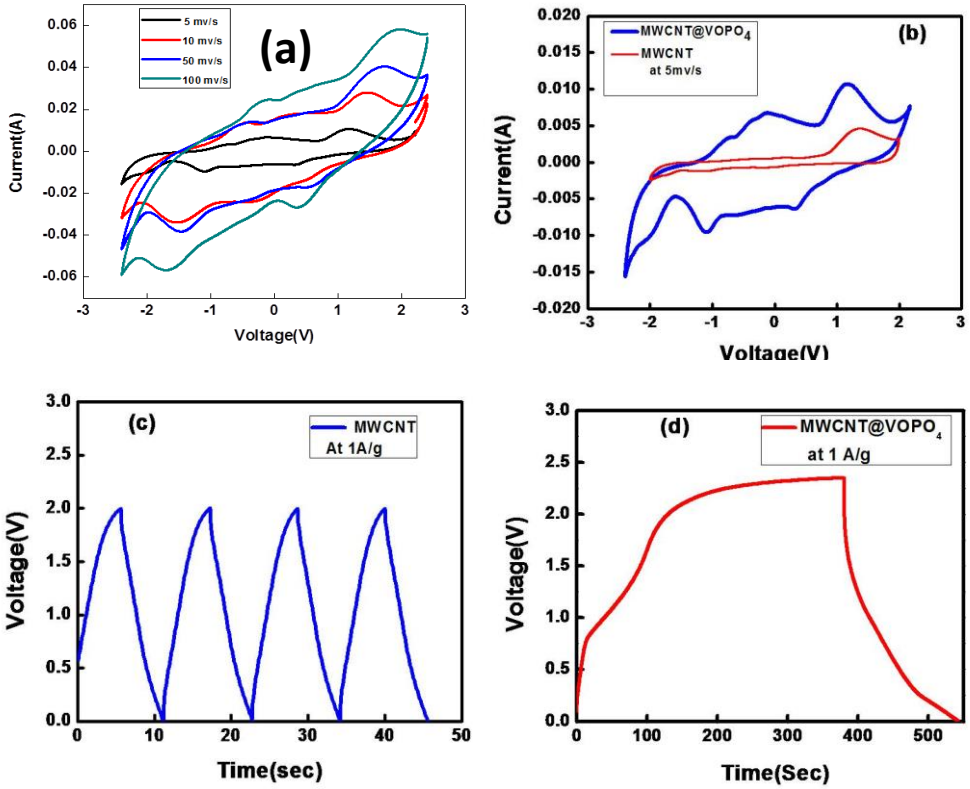

Figure 8.4. CV curves of hybrid electrodes at different scan rates (a), CV curves of MWCNT and hybrid electrodes at 5 mV/s(b),charging discharging curves of pure MWCNT(c) and hybrid electrodes(d) at 1 A/g

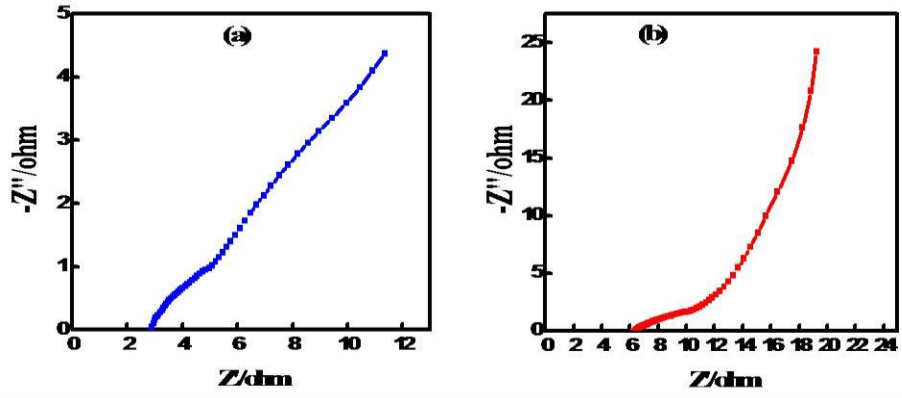

Figure 8.5. EIS plot of MWCNT electrodes (a), Hybrid electrodes (b)

We performed electrochemical impedance spectroscopy tests to evaluate the capacitive behavior of the supercapacitors. Fig. 8.5(a) and 8.5(b) shows Nyquist plots of MWCNT electrodes and hybrid electrodes respectively, where the ESR (equivalent series

resistance) for MWCNT electrodes and hybrid electrodes to be 2.9 ohm and 6 ohm respectively. The increase in series resistance of hybrid compare to only MWCNT film is obvious due to incorporation of $VOPO_4$. Higher the slope of the straight line at low frequency region in Nyquist plot implies better capacitive behavior of the devices. Here we can see from the figure 8.5(b) for hybrid film, the straight line at low frequency region in Nyquist plot is almost parallel to the imaginary axis, which indicates the ideal capacitive behavior of the supercapacitor based on MWCNT-$VOPO_4$ hybrid.

8.5 Summary

In summary, we have successfully synthesized vanadyl phosphate nano sheets in the simple exfoliation process. Further, to improve the electrochemical behavior MWCNT@$VOPO_4$ hybrid electrodes are prepared by vacuum filtering. The specific capacitance of hybrid electrodes was up to the 236 F/g at the scan rate 5 mV/s much higher than that of pure MWCNT electrodes (49 F/g) at the same scan rate. This MWCNT@$VOPO_4$ hybrid could be a good candidate for electrode of supercapacitor with superior energy efficiency.

8.6 .References

1. Xu Peng, Lele Peng, Changzheng Wu and Yi Xie, *Chem. Soc. Rev.*, 2014, **43**, 3303-3323.
2. H. Wang, H. S. Casalongue, Y. Liang and H. Dai, *J. Am.Chem. Soc.*, 2010, **132**, 7472–7477.
3. H. Shen, E.Liu, X.Xiang, Z.Huang, Y. Tian, Y.Wu, Z.Wu, H.Xie, *Mater.Res.Bull.*, 2012, **47**, 662-666.
4. A. Prakash, D. Bahadur, *ACS App. Mater. Inter.*, 2014, **6**, 1394-1405.
5. G. Wang, L. Zhang, J. Zhang, *Chem. Soc. Rev*. ,2012,**41**, 797-828.
6. S.L. Chou, J.Z. Wang, S.Y. Chew, H.K. Liu and S.X. Dou, *Electrochem. Commun.*, 2008, **10**, 1724–1727.
7. X. Lu, T. Zhai, X. Zhang, Y. Shen, L. Yuan, B. Hu, L. Gong, J. Chen, Y. Gao, J. Zhou, Y. Tong and Z. L. Wang, *Adv. Mater.*, 2012, **24**, 938–944.
8. J. Ge, G. Cheng and L. Chen, *Nanoscale*, 2011, **3**, 3084–3088.
9. Y. Sun, C. Wu, Y. Xie , *J Nanopart Res* , 2010, **12**, 417–427.
10. C. Wu, X. Lu, L. Peng, K. Xu, X. Peng, J. Huang, G. Yu and Y. Xie, *Nat. Commun.*, 2013, **4**, 3431.

11. D.Hanlon, C.Backes, T.M.Higgins, M.Hughes, A.O'Neill, P.King, N.McEvoy, G.S.Duesberg, B.M.Sanchez, H.Pettersson, V. Nicolosi, and J. N. Coleman, *Chem. Mater.*,2014, **26**,1751-1763.
12. L.Benes, K. Melanova, M. Trchova, P. Capkova, and P.Matejka, *Eur. J. Inorg. Chem.*, 1999, 2289-2294.
13. Z.Luo, E. Liu, T.Hu, Z.Li, T. Liu, *Ionics*, 2015, **21**,289-294.
14. G. Yu, L.Hu, M. Vosgueritchian, H. Wang, X. Xie, J. R. McDonough, X. Cui, Y. Cui, and Z. Bao, *Nano Lett.* ,2011, **11**, 2905-2911.
15. L. Peng, X. Peng, B. Liu, C. Wu, Y. Xie, and G. Yu, *Nano Lett*., 2013, **13**, 2151-2157.